11-1-2013

Timoshenko Beam Effects in Lateral-mode Microcantilever-based Sensors in Liquids

Joshua A. Schultz
Marquette University

Stephen M. Heinrich
Marquette University, stephen.heinrich@marquette.edu

Fabien Josse
Marquette University, fabien.josse@marquette.edu

Nicholas J. Nigro
Marquette University, nicholas.nigro@marquette.edu

Isabelle Dufour
Université de Bordeaux

See next page for additional authors

Accepted version. *Micro & Nano Letters*, Vol. 8, No. 11 (November 2013): 762-765. DOI.

Timoshenko Beam Effects in Lateral-Mode Microcantilever-Based Sensors in Liquids

Joshua A. Schultz
Department of Civil, Construction and Environmental Engineering
Marquette University
Milwaukee, WI
Stephen M. Heinrich
Department of Civil, Construction and Environmental Engineering
Marquette University
Milwaukee, WI
Fabien Josse
Department of Electrical and Computer Engineering
Marquette University
Milwaukee, WI
Nicholas J. Nigro
Department of Mechanical Engineering
Marquette University
Milwaukee, WI
Isabelle Dufour
CNRS, IMS Laboratory, Université de Bordeaux
Talence, France

Micro & Nano Letters, Vol 8, No. 11 (November 2013): pg. 762-765. DOI.

Luke A. Beardslee
School of Electrical and Computer Engineering
Georgia Institute of Technology
Atlanta, GA
Oliver Brand
School of Electrical and Computer Engineering
Georgia Institute of Technology
Atlanta, GA

Recent experimental and analytical research has shown that higher in-fluid quality factors (Q) are achieved by actuating microcantilevers in the lateral flexural mode, especially for microcantilevers having larger width-to-length ratios. However, experimental results show that for these geometries the resonant characteristics predicted by the existing analytical models differ from the measurements. A recently developed analytical model to more accurately predict the resonant behaviour of these devices in viscous fluids is described. The model incorporates viscous fluid effects via a Stokes-type fluid resistance assumption and 'Timoshenko beam' effects (shear deformation and rotatory inertia). Unlike predictions based on Euler-Bernoulli beam theory, the new theoretical results for both resonant frequency and Q exhibit the same trends as seen in the experimental data for in-water measurements as the beam slenderness decreases. An analytical formula for Q is also presented to explicitly illustrate how Q depends on beam geometry and on beam and fluid properties. Beam thickness effects are also examined and indicate that the analytical results yields good numerical estimates of Q for the thinner (5 μm) specimens tested, but overestimate Q for the thicker (20 μm) specimens, thus suggesting that a more accurate fluid resistance model should be introduced in the future for the latter case.

1. Introduction and motivation

Dynamic-mode microcantilevers are well suited to biological and chemical sensing applications. However, these applications often necessitate liquid-phase sensing, introducing significant fluid-induced inertial and dissipative forces which reduce resonant frequencies (f_{res}) and quality factors (Q) and, thus, adversely affect the sensitivity and the limit of detection. In an effort to mitigate these effects, unconventional resonant modes of microcantilevers have been investigated, one of which is the lateral flexural mode [1–4]. (The

Micro & Nano Letters, Vol 8, No. 11 (November 2013): pg. 762-765. DOI.

lateral flexural mode refers to bending vibrations in the plane of the microcantilever shown in Figure 1, as opposed to the more 'natural' out-of-plane vibrations.) Recent analytical [2, 3] and experimental [4] research has shown that higher in-fluid Q is achieved by employing this mode, which reduces the viscous energy dissipation in the fluid as compared with the transverse (out-of-plane) mode. In particular, both the theoretical and the experimental results show that the lateral-mode designs offering the most promise in liquids are those for which the microbeams are relatively short and wide. However, such geometries may violate the assumptions employed in Euler-Bernoulli (EB) beam theory because of the large width-to-length ratio. This is exhibited in the deviation between the EB predictions and the experimental data for f_{res} and Q for short, wide cantilevers, for which the EB theory overestimates the results [4].

To understand the behaviour of the lateral-mode devices in a better manner, a model that accounts for both fluid effects and 'Timoshenko beam' (TB) effects (shear deformation and rotatory inertia) is warranted. Recently, a TB/Stokes fluid resistance model was introduced by Schultz *et al.* [5] and was implemented in a primarily theoretical study to investigate the effects of the excitation method and detection scheme on the dynamic response of lateralmode microcantilevers [6]. However, in the latter study only a limited amount of experimental validation was performed; moreover, the appropriate specification of material input parameters to the model received minimal attention and the efficacy of the model with respect to cantilever thickness was not examined. To be useful for optimisation of the sensor geometries, the proposed model (or an appropriate extension) must be applicable over a sufficiently wide range of geometric parameters, including cantilever thickness. These issues are therefore the focus of the present Letter. More specifically, two methods of selecting material property input to the model are examined and discussed, and observations are made based on comparisons of model predictions and liquid-phase (water) experimental data. Recommendations based on these comparisons are made for future theoretical work.

Micro & Nano Letters, Vol 8, No. 11 (November 2013): pg. 762-765. DOI.

2. Assumptions

The major assumptions employed in the model are: (i) viscous dissipation in the fluid is the dominant loss mechanism; (ii) the cross-section is rectangular and relatively thin (thickness $h \ll$ width b), hence the fluid resistance associated with the pressure on smaller faces is negligible compared with the fluid's shear resistance on larger faces; and (iii) the shear stress exerted by the fluid on the beam is approximated by local application of the classical solution of Stokes's second problem for harmonic motion of an infinite rigid plate in a viscous fluid.

3. Boundary value problem

By modelling the microcantilever as a TB (e.g. [7]) with distributed Stokes-type fluid resistance [2, 3], two fourth-order partial differential equations (PDEs) which govern the total deflection, $\bar{v}$, and the rotation angle of the crosssection, φ, may be derived [8]. (The overbars denote the dimensionless quantities.) Separation of the variables leads to two ordinary differential equations (ODEs) for the spatially dependent deflection and rotation fields, $\bar{V}(\xi)$ and $\Phi(\xi)$, where $\xi = x/L$ is a normalised coordinate and *i* is the imaginary unit

$$\bar{V}'''' + \lambda^3 (r^2 + s^2)[\lambda + (1 - i)\zeta]\bar{V}'' - \lambda^3[\lambda + (1 - i)\zeta]\{1 - r^2 s^2 \lambda^3[\lambda + (1 - i)\zeta]\}\bar{V} = 0 \quad (1)$$

$$\Phi''' + \lambda^3(r^2 + s^2)[\lambda + (1 - i)\zeta]\Phi'' - \lambda^3[\lambda + (1 - i)\zeta]\{1 - r^2 s^2 \lambda^3[\lambda + (1 - i)\zeta]\}\Phi = 0, \quad (2)$$

Quantities $\bar{V}$ and Φ are, respectively, the complex amplitudes of the total beam deflection (bending plus shear) and the rotation angle. The ODEs (and the corresponding PDEs) involve four independent dimensionless parameters: r, s, λ and ζ. The TB parameters, r and s, are defined as the rotational inertia parameter, $r^2 \equiv I/AL^2$, and the

Micro & Nano Letters, Vol 8, No. 11 (November 2013): pg. 762-765. DOI.

shear deformation parameter, $s^2 \equiv \mathrm{EI}/kAGL^2$, where A and I are the cross-section's area and second moment of area, E and G are the effective Young's modulus and shear modulus, k = 5/6 is the shear coefficient and L is the beam length. Parameters λ and ζ are the frequency and the fluid resistance parameters, which are related to the fundamental system parameters by

$$\lambda \equiv \left(\frac{12\rho_b L^4 \omega^2}{Eb^2}\right)^{1/4} \tag{3}$$

$$\zeta \equiv \frac{L}{hb^{1/2}}\left(\frac{48\rho_f^2 \eta^2}{E\rho_b^3}\right)^{1/4} \tag{4}$$

where ρ_b is the beam density and ρ_f and η are the fluid density and viscosity. Parameter ω is the driving/response frequency (rad/s), so that λ is a dimensionless excitation/response frequency. (The corresponding excitation/response frequency, f, in Hz is given by $f = \omega/2\pi$.) The imposed boundary conditions correspond to electrothermal harmonic excitation via integrated heating resistors near the base of the cantilever (Figure 1) and are given by Schultz [8]

$$\bar{V}(0) = 0 \tag{5}$$

$$\Phi(0) = \theta_0 \tag{6}$$

$$\Phi'(1) = 0 \tag{7}$$

$$\bar{V}'(1) - \Phi(1) = 0 \tag{8}$$

where θ_0 represents the amplitude of the 'effective support rotation' imparted by the heating resistors [3].

Micro & Nano Letters, Vol 8, No. 11 (November 2013): pg. 762-765. DOI.

4. Results and discussion

The boundary value problem defined by (1,2) and (5)–(8) was solved analytically and the results expressed in terms of two 'output signals': total tip displacement and bending tip displacement, corresponding respectively to the optical and piezoresistive detection methods [8]. Both f_{res} and Q were extracted from the theoretical beam response and were found to be insensitive to the output signal type for fluid resistance values in the range $0 \leq \zeta \leq 0.3$, which includes values associated with all the specimens tested [5].

Given the importance of Q in liquid-phase microcantilever resonator applications, a surface-fitting procedure was applied to the theoretical results to obtain the following analytical formula, which explicitly shows how Q depends on the system parameters

$$Q \approx 0.7124 \frac{hb^{1/2}}{\mathrm{L}} \left(\frac{\mathrm{E}\rho_b^3}{\rho_f^2 \eta^2} \right)^{1/4} \mathrm{X} \left[1 - 0.0789 \left(\frac{b}{L}\right)^{2.529} - 0.0721 \left(\frac{b}{L}\right)^{1.578} \left(\frac{E}{G}\right)^{0.823} \right] \quad (9)$$

The bracketed expression represents a correction factor associated with TB effects, which reduces the EB result [2] appearing in front of the correction factor. The results of (9) are within 2.0% of those generated by the current analytical model over the following practical ranges of parameters: $\zeta \in [0, 0.05]$, $r \in [0, 0.2]$ and $\sqrt{E/kG} \in [[0, 3]$.

To generate numerical results from the current TB model it is necessary to specify the values of the effective elastic properties of the microbeam (E and G). Owing to the composite nature of the cantilevers modelled in this study (Si base layer plus several passivation layers [8]), it is problematic to specify appropriate values of these effective moduli; therefore one method that was utilized to specify these values was based on fitting the in-vacuum resonant

Micro & Nano Letters, Vol 8, No. 11 (November 2013): pg. 762-765. DOI.

frequency results of the present model to in-air experimental data, assuming that the air resistance has a negligible effect on f_{res}. The fitting procedure was formulated in such a manner that the fitting parameters were taken to be $C_1 \equiv \sqrt{E/12\rho_b}$ and $C_2 \equiv \sqrt{E/kG}$. (Since k = 5/6 and the beam density is typically known, the determination of C_1 and C_2 is equivalent to determining E and G.) Relevant device geometries and the fitting procedure are described elsewhere [6, 8]. The values of C_1 and C_2 as determined by the fitting method are shown in Table 1 along with the back-calculated values of E, assuming that ρb = 2330 kg/m^3 (silicon). These values were then used as input to the model when making comparisons between the theoretical in-water results and the in-water test data (the comparison of the main interest in this study). A second method for specifying the C_2 value was to choose C_2 = 2 for all cases as this is the 'textbook value' based on a standard (100) silicon wafer with the microcantilever oriented along the [110] axis, that is, E = 169 GPa and G = 50.9 GPa [9]. This second method for specifying C_2 was motivated by the fact that the first method yielded values for E/G that seemed to be unrealistically large for a structure that is primarily silicon.

Table 1 shows that E obtained from the C_1 values follows a decreasing trend as the thickness increases. A possible explanation for this behaviour is that, as the actual stiffness of the beam increases (via increasing thickness), the effects of support compliance may be increasing. (Support compliance in these types of structures has been modelled in detail and the results support this hypothesis [10, 11].) Consequently, the overall system has a decreasing stiffness which is indirectly accounted for here through a reduced value of E.

The results shown in Figures 2 and 3 for the thinnest specimen set (nominal thickness h_{nom} = 5 μm) indicate that the model is capable of matching the experimental data quite well for both f_{res} and Q for lateral-mode microcantilevers at higher b/L ratios (i.e. for the high-Q devices for which the EB models prove inadequate).

Micro & Nano Letters, Vol 8, No. 11 (November 2013): pg. 762-765. DOI.

However, these Figures are based on the C_2 values of Table 1 which, as indicated above, are most probably underestimating the actual shear modulus G. Consequently, the second method of generating the theoretical results, based on specifying C_2 = 2 (with C_1 as given in Table 1), was used. These results are compared in Figures 4 and 5 with the same dataset ($h$nom = 5 μm) as in Figures 2 and 3. Although the model still simulates the qualitative softening trend of the data for the 'stubbier' specimens, the magnitude of the softening is significantly underestimated, unlike in Figures 2 and 3. The likely reason is that the larger C_2 values used in the earlier Figures are indirectly incorporating the influence of support flexibility, whereas the approach used to generate Figures 4 and 5 does not.

To examine the influence of cantilever thickness on resonant characteristics, comparisons of the theoretical predictions and experimental data were also performed for the case of h_{nom} = 20 μm, again using C_2 = 2. Figures 6 and 7 illustrate that, while the current theory accurately models the trends in both f_{es} and Q at higher b/L ratios, there is a tendency for the current model to overestimate Q more for the thicker specimens. This is probably associated with a breakdown of the assumption that the effect of fluid pressure on the smaller faces of the beam is negligible. As the thickness increases, the pressure effects will become more important and should be incorporated into future modelling efforts.

Over the practical ranges of the system parameters considered, the theoretical results indicate that the TB effects can account for a reduction in f_{res} and Q of up to ~ 40 and ~ 25%, respectively, but have effects of less than 2% when $L/b > 10$. The improved frequency estimates are smaller than the EB results because the TB model has lower stiffness (because of shear deformation) and greater mass (because of rotatory inertia), thereby causing a departure from the linear EB frequency results (Figures 2, 4 and 6). Similar conclusions apply to the Q comparisons among the experimental data and the TB and EB models (Figures 3, 5 and 7), although the departure from linearity is of smaller magnitude than for the frequency results.

Micro & Nano Letters, Vol 8, No. 11 (November 2013): pg. 762-765. DOI.

In summary, the TB model presented here for lateral-mode cantilevers captures the trends in liquid-phase experimental data more accurately than the existing EB models. In addition, an analytical equation has been presented to explicitly show the relationship between Q and the geometric and material parameters of the microcantilever/fluid system, which may serve as an aid in both preliminary design and device optimisation. In particular, the present model has important implications from the sensors design standpoint since the ability to accurately relate resonant frequency and Q to design and fluid parameters is a critical first step in understanding how to design for desired levels of performance (i.e. sensitivity and limit of detection). Ongoing modelling efforts involve more complete parametric studies on both resonant characteristics and sensor performance metrics. Generalisations of the model to incorporate the effects of support compliance and more complex beam/fluid interaction are also being pursued for applications involving thicker lateral-mode devices.

5. Acknowledgment

This work is supported in part by NSF grant nos ECCS-0824017 and ECCS-1128992.

6 References

[1] Sharos L.B., Raman A., Crittenden S., Reifenberger R.: 'Enhanced mass sensing using torsional and lateral resonances in microcantilevers', Appl. Phys. Lett., 2004, 84, pp. 4638–4640

[2] Heinrich S.M., Maharjan R., Beardslee L., Brand O., Dufour I., Josse F.: 'An analytical model for in-plane flexural vibrations of thin cantilever-based sensors in viscous fluids: applications to chemical sensing in liquids'. Proc. Int. Workshop on Nanomechanical Cantilever Sensors, Banff, Canada, 2010, p. 2

[3] Heinrich S.M., Maharjan R., Dufour I., Josse F., Beardslee L.A., Brand O.: 'An analytical model of a thermally excited microcantilever vibrating laterally in a viscous fluid'. Proc. IEEE Sensors, Conf., 2010, Waikoloa, Hawaii, pp. 1399–1404

[4] Beardslee L.A., Josse F., Heinrich S.M., Dufour I., Brand O.: 'Geometrical considerations for the design of liquid-phase biochemical sensors using

a cantilever's fundamental in-plane mode', Sens. Actuators B, 2012, 164, pp. 7–14

[5] Schultz J.A., Heinrich S.M., Josse F., ET AL.: 'Timoshenko beam effects in lateral-mode microcantilever-based sensors in liquids'. Proc. Int. Workshop on Nanomechanical Sensing, Stanford, CA, USA, 2013, pp. 143–144

[6] Schultz J.A., Heinrich S.M., Josse F., ET AL.: 'Timoshenko beam model for lateral vibration of liquid-phase microcantilever-based sensors'. Proc. SEM 2013 Annual Conf. and Exposition on Experimental and Applied Mechanics, Lombard, IL, USA, 2013, p. 10

[7] Timoshenko S., Young D.H.: 'Vibration problems in engineering' (Van Nostrand, New York, 1955, 3rd edn) [8] Schultz J.A.: 'Lateral-mode vibration of microcantilever-based sensors in viscous fluids using Timoshenko beam theory'. Doctoral Dissertation, Marquette University, Milwaukee, WI, USA, 2012

[9] Hopcroft M.A., Nix W.D., Kenny T.W.: 'What is the Young's modulus of silicon?', J. Microelectromech. Syst., 2010, 19, pp. 229–238

[10] MacBain J.C., Genin J.: 'Effect of support flexibility on the fundamental frequency of vibrating beams', J. Franklin Inst., 1973, 296, pp. 259–273

[11] Maharjan R.: 'Effect of support compliance on the resonant behavior of microcantilever-based sensors in viscous fluids'. Doctoral Dissertation, Marquette University, Milwaukee, WI, USA, 2013

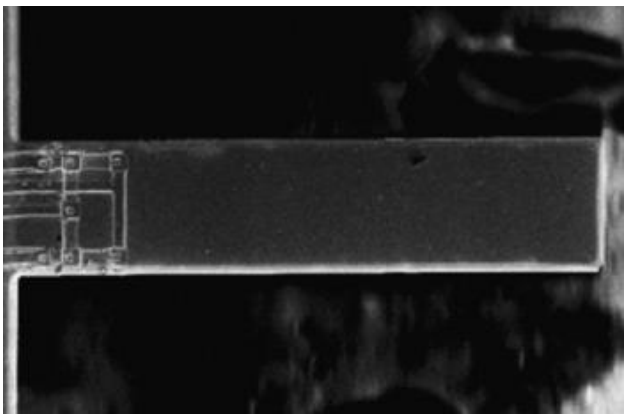

Figure 1 Microcantilever with heating resistors near support to excite lateral (in-plane) bending [4]

Micro & Nano Letters, Vol 8, No. 11 (November 2013): pg. 762-765. DOI.

Nominal thickness, h_{nom}, μm	C_1, km/s	C_2	E, GPa
5	2.324	4.423	151.0
8	2.190	3.512	134.1
12	2.192	3.129	134.3
20	2.145	3.064	128.6

Table 1 C_1 and C_2 based on fitting the in-vacuum model to the in-air frequency data (E obtained from C_1)

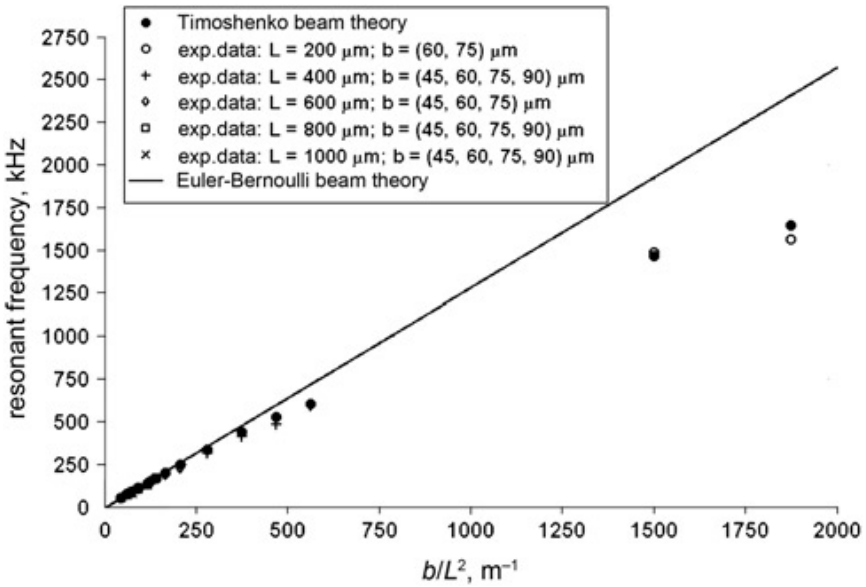

Figure 2 Resonant frequency comparison (in water, h = 7.02 μm, C_2 = 4.423): current model, EB model and experimental data

Micro & Nano Letters, Vol 8, No. 11 (November 2013): pg. 762-765. DOI.

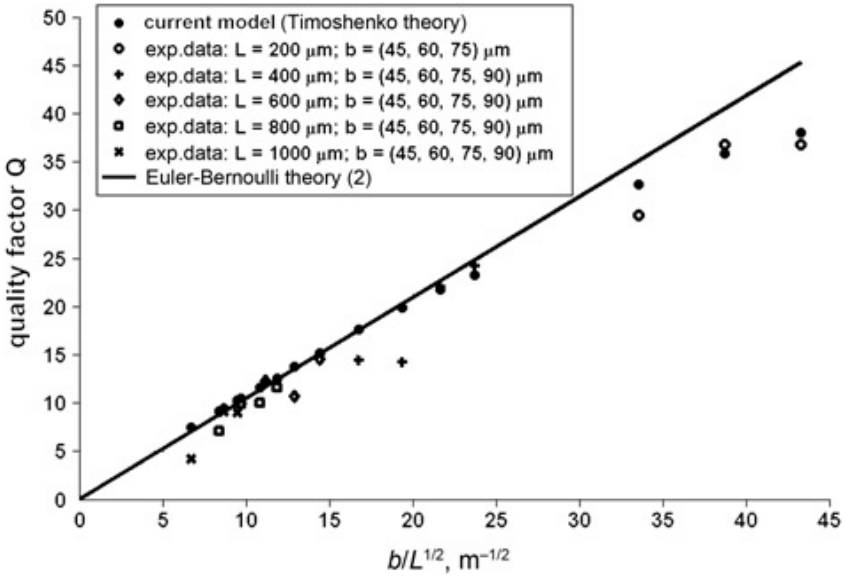

Figure 3 Quality factor comparison (in water, h = 7.02 μm, C_2 = 4.423): current model, EB model and experimental data from [4]

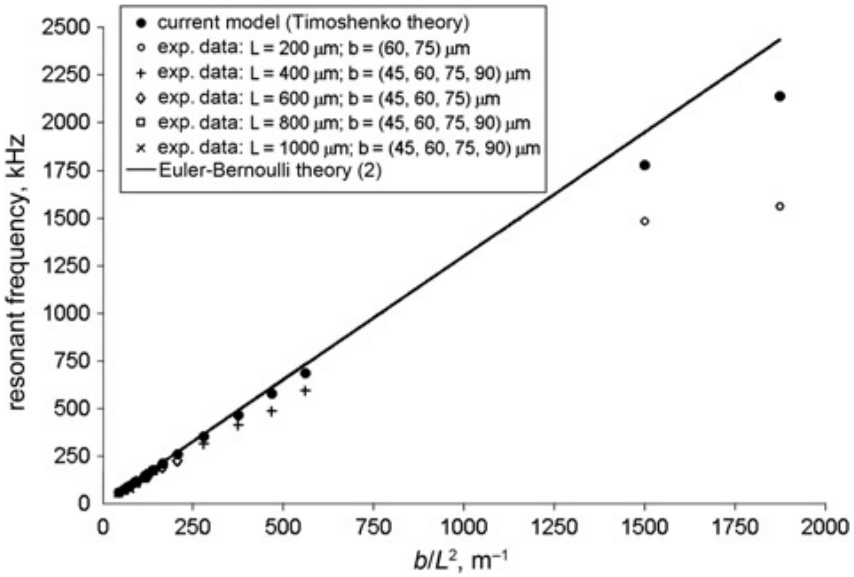

Figure 4 Resonant frequency comparison (in water, h = 7.02 μm, C_2 = 2): current model, EB model and experimental data

Micro & Nano Letters, Vol 8, No. 11 (November 2013): pg. 762-765. DOI.

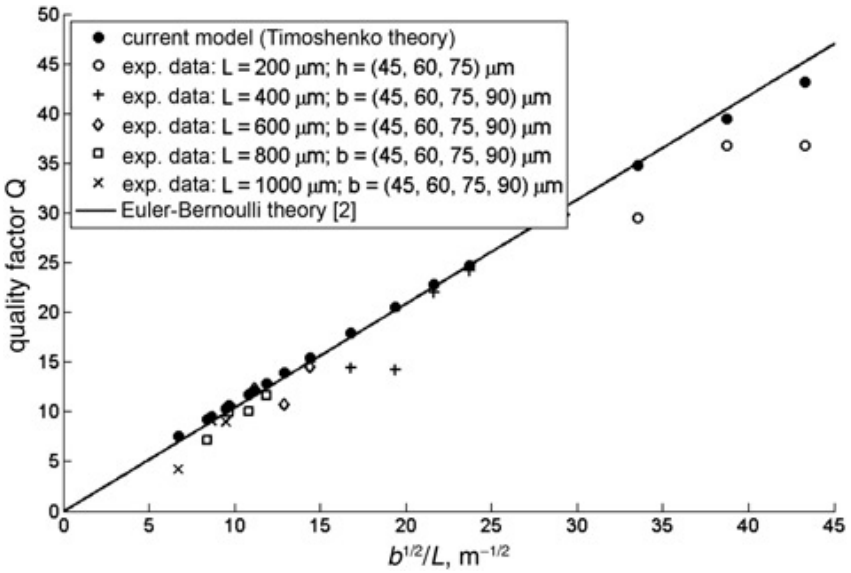

Figure 5 Quality factor comparison (in water, h = 7.02 μm, C_2 = 2): current model, EB model and experimental data from [4]

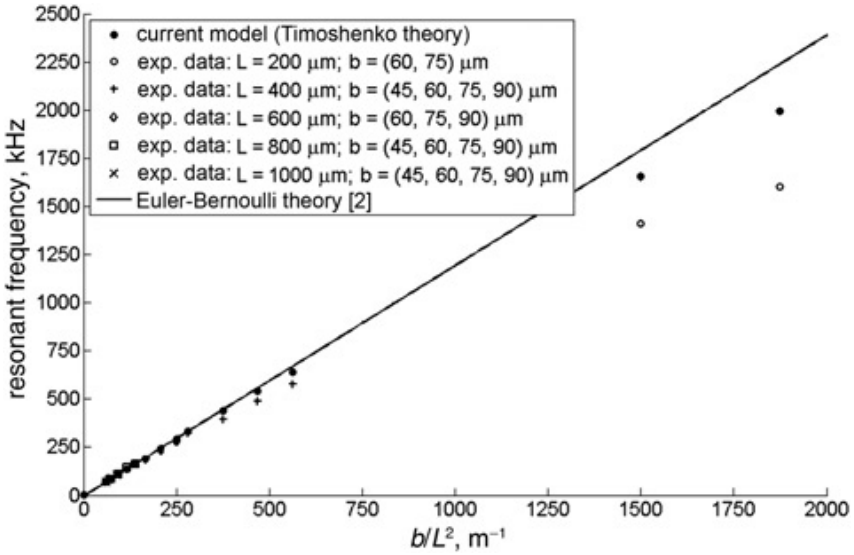

Figure 6 Resonant frequency comparison (in water, h = 22.34 μm, C_2 = 2): current model, EB model and experimental data

Micro & Nano Letters, Vol 8, No. 11 (November 2013): pg. 762-765. DOI.

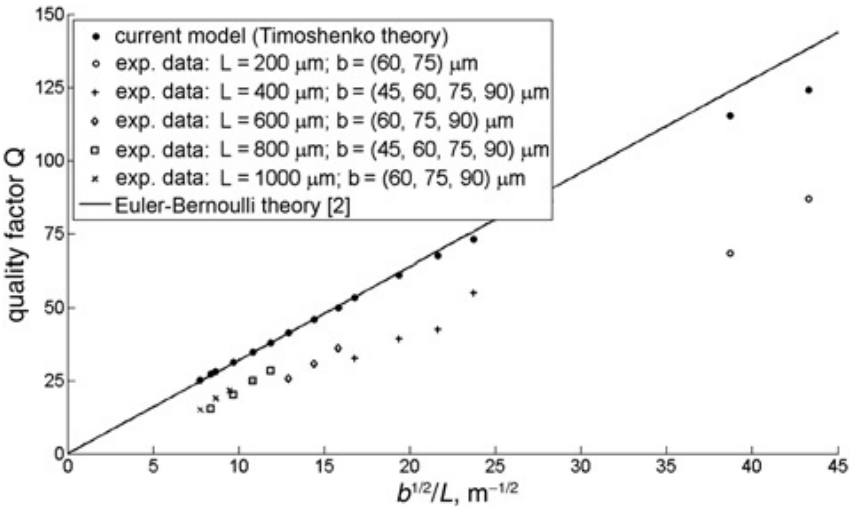

Figure 7 Quality factor comparison (in water, h = 22.34 μm, C_2 = 2): current model, EB model and experimental data from [4]

Micro & Nano Letters, Vol 8, No. 11 (November 2013): pg. 762-765. DOI.